



## Thermal conductivity of archaeological ceramics: The effect of inclusions, porosity and firing temperature

Anno Hein<sup>a,\*</sup>, Noémi S. Müller<sup>a,b</sup>, Peter M. Day<sup>b</sup>, Vassilis Kilikoglou<sup>a</sup>

<sup>a</sup> Institute of Materials Science, N.C.S.R. "Demokritos", Aghia Paraskevi, 15310 Athens, Greece

<sup>b</sup> Department of Archaeology, University of Sheffield, Northgate House, West Street, Sheffield S1 4ET, UK

### ARTICLE INFO

#### Article history:

Received 11 March 2008

Received in revised form 2 September 2008

Accepted 15 September 2008

Available online 24 September 2008

#### Keywords:

Archaeological cooking pots

Temper material

Thermal properties

Heat transfer

### ABSTRACT

In former studies on archaeological cooking pots or archaeological pyrotechnical ceramics their thermal conductivity was discussed only in relation with other parameters but, it was never actually determined. In the present study a modified Lees' disk setup was used in order to determine the thermal conductivity of a series of experimental ceramic disks. As for the manufacture of these disks typical ceramic fabrics were simulated, which can be observed in archaeological cooking pots. In order to assess the effect of production parameters on the thermal conductivity, two different clays, one non-calcareous and one calcareous, were tempered with different amounts of granite or phyllite and were fired at three different temperatures: 550 °C, 850 °C and 1050 °C. The most important parameters emerged as the degree of vitrification and porosity of the ceramic matrix.

© 2008 Elsevier B.V. All rights reserved.

### 1. Introduction

Ceramics are among the first composite materials manufactured and used by humans. Even from early times, through the selection of particular raw materials, modification of the clay paste, creation of specific shapes and the application of suitable firing conditions, the material properties of the end product were controlled and ceramic ware types suitable for specific applications were fabricated. In particular applications, the properties of heat resistance or heat capacity were extremely beneficial. For certain ware types, such as cooking vessels or technical ceramics used in metal and glass production, these were important performance parameters. Depending on their function, however, different ware types required fundamentally different material properties concerning their thermal conductivity. In the case of cooking pots, for example, high thermal conductivity was beneficial, allowing easier heating of the vessel's contents. Moreover, thermal gradients in the vessels' walls were reduced, preventing thermal shock. The same applied to certain functional types of metallurgical ceramics, such as crucibles used with an external heating source, whereas smelting furnaces, which were heated from inside, were constructed instead to be insulating [1]. Therefore, the question arises: how and to what extent could the different requirements in terms of thermal conductivity be met by varying the production parameters?

The adaptation of archaeological pottery to fulfil different use requirements has been discussed with regard to material properties and specialisation, usually focusing on strength and toughness [2]. Occasionally, thermal shock resistance [3] and cooling properties [4] have been investigated as well. Less consideration has been given to the thermal conductivity of the ceramic material until now, although this is an important parameter especially when ceramics are used at high temperatures. The latter has been discussed only in relation to the wall thickness of the ceramic vessels [5–7]. In an approach to quantify heat transfer in cooking pots, the parameter 'heating effectiveness' was defined as the rate the temperature of the pot's content is raised by applying an external heat source under controlled conditions [4,8,9]. This parameter, however, is a complex product of heat conductivity, heat flux, heat capacity, permeability and shape of the vessels. Recently, in order to estimate their energy consumption, the thermal efficiency of traditional cooking vessels in Iran, albeit non-ceramic, was estimated in relation to different vessel parameters using a mathematical model [10]. Thermal efficiency described the ratio between the energy needed to heat and partially boil a certain mass of water and the heat energy applied for this reason with gas flame.

In comparison to cooking pots, heat transfer in pyrotechnical ceramics has been investigated more systematically, mainly in view of the operation conditions of smelting furnaces [11,12]. The thermal conductivity of archaeological ceramics, however, has never been measured in a straightforward manner, but instead reference values of ceramics have been used. In most studies of pyrotechnical ceramics the selection of raw materials, the addition of various

\* Corresponding author.

E-mail address: [hein@ims.demokritos.gr](mailto:hein@ims.demokritos.gr) (A. Hein).

non-plastic or organic tempers and the ceramic matrix developed, were interpreted in terms of the ceramics' refractoriness [12,13]. Only recently the influence of porosity and particularly of the orientation of porosity on the thermal conductivity of smelting furnaces was investigated using computer models of the ceramic matrix.

In the present paper a simple approach for determining the thermal conductivity of archaeological ceramics is presented. This approach has been applied to a series of laboratory samples which were fabricated in order to reproduce typical archaeological cooking pot fabrics. The study of laboratory replicas has several advantages: firstly, the production of multiple test specimens from archaeological ceramics is practically impossible due to restrictions in sampling and deterioration of the ceramics during burial. Secondly, replicas provide a better control over specific parameters under study, covering a large spectrum of fabrics based on archaeological evidence. The aim of this study was to investigate the influence of various parameters, such as type, shape and amount of inclusions and firing temperature, on thermal conductivity. This information in turn can offer valuable criteria for the ongoing discussion over the extent to which technological changes in archaeological pottery production are connected with intentional improvements in the performance of the vessels.

## 2. Heat transfer in ceramics: parameters influencing thermal conductivity

As far as archaeological ceramics are concerned, the main heat transfer process, which will be focussed on in the present paper, is heat conduction. Heat convection, which is the heat transfer between a solid surface and a moving fluid, such as water in a cooking pot or the ambient air around pyrotechnical ceramics has to be considered only at the ceramic surfaces [1]. Heat transfer by radiation can be neglected because at the assumed temperatures used for cooking, or even in metallurgical applications, the contribution of heat radiation is still small compared to the other heat transfer processes.

The heat transfer in solid materials by heat conduction depends on the thermal conductivity  $k$  of the specific material. This material parameter describes the heat flux  $dQ/dt$  normal to an area  $A$  under a particular temperature gradient  $\nabla T$  [14]. In the case of earthenware ceramics, thermal conductivity typically lies in the range of  $0.5\text{--}1.5\text{ W (m K)}^{-1}$  normally with decreasing values at higher temperatures [15]. For solid materials with crystal structure, possible anisotropy of the thermal conductivity has to be considered as well.

In the case of non-static temperature conditions the heat transfer is described with the heat conduction equation [14]:

$$\frac{\partial T}{\partial t} = \alpha \cdot \nabla^2 T \quad (1)$$

In this equation the so-called thermal diffusivity  $\alpha$  is the quotient between the thermal conductivity  $k$  and the heat capacity per unit volume  $\rho c_p$ .

Archaeological ceramics, even when they appear to be of fine nature, are complex composites. The base material, the actual ceramic matrix, is a mixture of different clay minerals, high temperature phases, non-plastic inclusions (either natural components of the raw material or intentionally added temper, such as quartz, feldspars, carbonates, micas or rock fragments) and finally various kinds of pores and voids. Therefore, regarding their material properties, archaeological ceramics can be described as multiphase composites. Some of the material properties, such as effective heat capacity  $c_{p,eff}$  or effective density  $\rho_{eff}$ , can be estimated in a straightforward fashion as the sum of the values of the particular phases multiplied by their respective volume fractions. The effective heat conductivity  $k_{eff}$ , however, depends additionally on

the geometrical arrangement of the phases [14]. Therefore, apart from the volume fraction of different non-plastic inclusions and pores, also their size, shape and orientation affect the thermal conductivity of the ceramics. In particular, porosity  $\Pi$  affects the thermal conductivity, as the pores act as heat barriers. In order to estimate  $k_{eff}$ , theoretical models can be applied [15] or, based on the ceramic's microstructure, computer models can be evaluated with the finite element method [1]. In the case of randomly distributed and oriented pores  $k_{eff}$  can be estimated with the following formula [15]:

$$\frac{k_{eff}}{k_{solid}} = (1 - \Pi)^{3/2} + \Pi^{1/4} \frac{k_{por}}{k_{solid}} \quad (2)$$

with  $k_{solid}$ , the thermal conductivity of the solid part, and  $k_{por}$ , the thermal conductivity of the pores.

## 3. Analytical method

For the determination of the thermal conductivity of ceramic samples within a temperature range of  $50\text{--}400^\circ\text{C}$  a modified Lees' disk setup was used. This rather simple method is particularly suitable for insulating materials. The examined sample in the shape of a flat disk is in contact with a heat source at one side and with a heat conductor at the opposite side. During the measurement the temperature of the heat source is controlled and stabilized. The heat loss of the heat conductor into the environment in relation to the particular temperature  $\dot{q}_{loss}(T)$  is estimated before the actual experiment with a reasonable accuracy, while the heat loss from the rim of the sample disk can be neglected provided that this is small compared to its diameter. In this way the heat flux through the sample can be determined. When steady state is reached, the temperature difference between heat source and ceramic surface in contact with the heat conductor  $dT = T_0 - T_{surf}$  provides the thermal conductivity of the ceramic taking into account the area and the thickness of the sample:

$$k(T) = \dot{q}_{loss}(T) \frac{x}{A dT} \quad (3)$$

The slope of the heating curve and particularly the time after which steady state is reached depend on the thermal diffusivity of the ceramics. The higher  $\alpha$ , the faster the temperature increases and equilibrium is reached.

In the present work the samples were heated from one side with a heating plate in combination with a thermostat (XENON TSL 100 with P/I controller). The temperature of the heating plate was controlled electronically within a range of approximately  $\pm 0.2^\circ\text{C}$ , monitored with a K-type thermocouple attached to the heating plate, and it could be freely chosen up to  $400^\circ\text{C}$ . The opposite surface of the sample was attached to a brass disk whose temperature was monitored with a second K-type thermocouple. Both thermocouples were connected to a data logger, so that the temperature development during the whole measurement could be recorded (Fig. 1). During the measurements, the ambient temperature was monitored and possible draughts were restrained in order to provide consistent experimental conditions.

The heat loss of the brass disk was determined by heating it up to a temperature of  $400^\circ\text{C}$  and afterwards leaving it to cool down while recording its temperature. During cooling, the surface which is in contact with the sample during a normal measurement was placed on a thermal insulator. Therefore, with the measured temperature decay the heat flux  $\dot{q}_{loss}(T)$  from the brass disk to the environment at specific temperatures can be determined:

$$\dot{q}_{loss}(T) = m_{brass} c_{p,brass} \frac{dT}{dt} \quad (4)$$

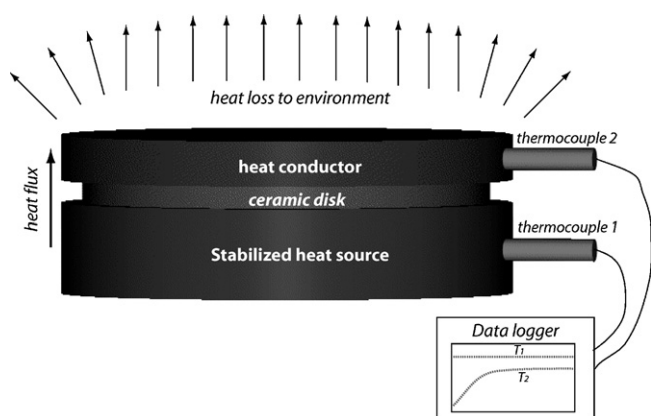


**Fig. 1.** Schematic diagram of the experimental setup. The ceramic disk is placed between a stabilized heat source and a heat conductor. The temperatures of heat source  $T_1$  and conductor  $T_2$  are recorded with thermocouples connected to a data logger.

The heat capacity of the brass disk was determined as  $0.366 \pm 0.010$  kJ/(kg K) and the weight was  $225.5 \pm 0.1$  g. With the slope of the time/temperature curve, the heat loss to temperature dependence was determined (Fig. 2).

With regard to the measured temperature differences in steady state, the heat transfer by heat radiation between heating plate and heat conductor was estimated as at most 2% of  $\dot{q}_{loss}(T)$ , so that it could be neglected. During the heating phase, however, the effect of heat radiation was larger in terms of accelerated temperature increase of the heat conductor. Therefore, it was not possible to determine directly the thermal diffusivity of the ceramic disk from the heating curve.

#### 4. Experimental ceramic disks

In order to investigate different parameters of ceramic production, particularly in view of cooking ware, a series of test specimens was fabricated to be examined for their thermal conductivity. Based on existing evidence concerning common archaeological cooking ware fabrics, two different base clays were selected for the fabrication of the test specimens: a calcareous clay from Pikermi (Attiki, Greece), which has been already used for systematic studies of mechanical properties [16] and a non-calcareous clay from Kalami (Crete, Greece). From both raw materials, fractions with a particle size of  $<30 \mu\text{m}$  were separated. Chemical compositions of the base clays determined by SEM-EDS are presented in Table 1. The analyses

**Table 1**

Chemical compositions of the two base clays according to SEM-EDS. The concentrations are given in wt%.

	Pikermi	Kalami
Na <sub>2</sub> O	0.9	1
MgO	1.9	1
Al <sub>2</sub> O <sub>3</sub>	20.3	19.8
SiO <sub>2</sub>	50.3	65
P <sub>2</sub> O <sub>5</sub>	0.9	0.6
SO <sub>3</sub>	0.4	0.2
Cl <sub>2</sub> O	<0.1	<0.1
K <sub>2</sub> O	2.6	2.5
CaO	14	0.5
TiO <sub>2</sub>	0.7	1.2
MnO	0.1	n.d.
Fe <sub>2</sub> O <sub>3</sub>	8	8.3

were performed in a FEI-Quanta Inspect SEM using carbon-coated polished sections of non-tempered specimens that were fired at 1050 °C, while freshly fractured carbon-coated surfaces were used for the study of microstructure. Furthermore, the base clays were examined with XRD, using a Siemens D 500 diffractometer with Cu-K<sub>α</sub> source. According to semi-quantitative evaluation of the XRD analysis of the unfired clays using the reference intensity ratio method [17], Kalami clay (KAL) was purely illitic with considerable amounts of quartz and feldspar and traces of hematite. Pikermi clay (PIK), apart from the above phases, showed additionally chlorite and the expected amount of calcite (>20% CaCO<sub>3</sub>). Each of the two base clays was mixed with two different types of temper materials, known to have been used in cooking pot production in the Aegean Bronze Age: granite and phyllite, which for the purpose of the present study were collected from the island of Naxos (Greece) and from Northeast Peloponnese (Greece), respectively. The mineralogical composition of the platy shaped phyllite was determined by XRD as follows: quartz, muscovite, chlorite and traces of hematite. Even though graphite could not be detected, perhaps due to its poor crystallinity, the dark colour of the phyllite as well as its grey streak indicated the presence of graphite as well. Both materials were crushed and fractions with a particle size of 0.5–1.0 mm were separated. Mixtures with an amount of temper material of 10 wt% and 40 wt% were prepared, resulting in 10 different clay mixtures (Table 2). From each clay mixture three disk shaped samples were prepared using a PVC mould (diameter: 58 mm, height: ca. 8 mm). For the preparation of the phyllite tempered clay disks, the clay was repeatedly folded and flattened, in order to obtain a preferred orientation of the platy phyllite particles parallel to the surface of the disks, imitating common archaeological fabrics.

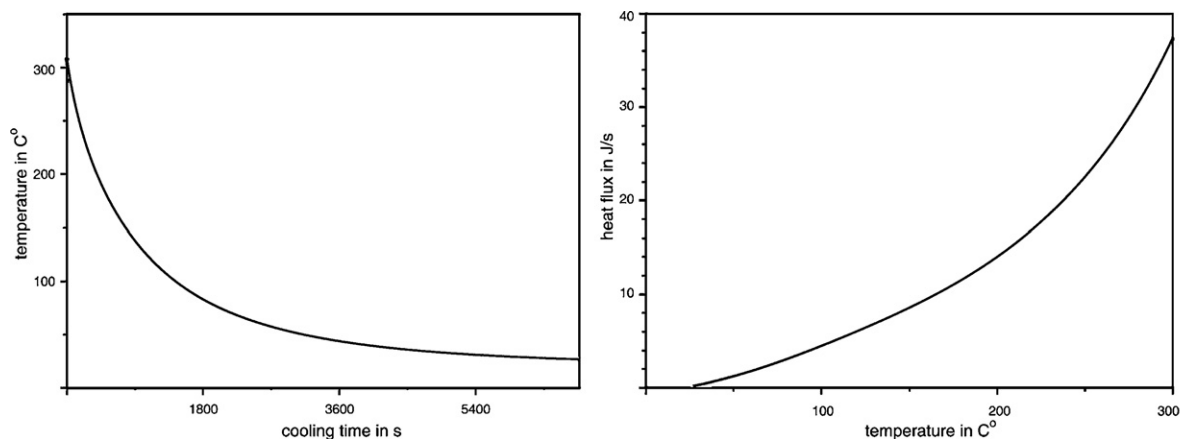


**Fig. 2.** Cooling curve of the brass plate at an ambient temperature of 25 °C (left) and estimated heat flux in relation to temperature (right).

**Table 2**  
Clays used for the experimental ceramic disks.

	Base clay	Temper
PIK-UT	Calcareous	Untempered
PIK-G10	Calcareous	10% granite
PIK-G40	Calcareous	40% granite
PIK-P10	Calcareous	10% phyllite
PIK-P40	Calcareous	40% phyllite
KAL-UT	Non-calcareous	Untempered
KAL-G10	Non-calcareous	10% granite
KAL-G40	Non-calcareous	40% granite
KAL-P10	Non-calcareous	10% phyllite
KAL-P40	Non-calcareous	40% phyllite

The clay disks were then fired at three different temperatures, 550 °C, 850 °C and 1050 °C, with heating rates of 200 °C/h and soaking times of 1 h in oxidizing atmosphere. XRD analysis of the fired clay mixtures indicated that at 850 °C most of the clay minerals were decomposed apart from illite, which still was present, albeit in a lower amount. In the Pikermi samples the calcite was decomposed, while gehlenite and wollastonite were formed. At 1050 °C diopside and anorthite were formed instead. Finally, in all samples the hematite peaks became more intense at higher temperatures, furthermore in the Kalami-based clay mixtures mullite was forming at 1050 °C.

With regard to the known effect of porosity on thermal conductivity, open and closed porosity of the fired ceramics were measured by water immersion according to standard methods [18]. The theoretical true density of the two base clays was determined as the sum of the values of the constituent phases multiplied by their estimated volume fractions, calculated from the weight fractions as determined by XRD. In this way the true densities were estimated as  $2.77 \pm 0.05$  g/ml for the non-tempered Kalami clay and  $2.68 \pm 0.05$  g/ml for the non-tempered Pikermi clay. Table 3 lists the measured apparent density and the total porosity of the different fabrics, considering the effect of temper materials on the density and assuming that the true density did not change considerably during firing. A comparison with the measured open porosity indicated noticeable closed porosity only for the case of high fired Kalami-based mixtures.

For the thermal conductivity determinations, a total of 30 different ceramic disks were measured at temperatures in a range of 50–300 °C with the modified Lee's device, described above. In order to ensure good contact between the ceramic disks and the hot plate as well as the heat conductor the surfaces were ground flat and in the case of flaws a conductive paste was applied.

## 5. Results and discussion

At a first stage, the reproducibility of the experimental setup was evaluated. Repeated measurements of the same disks at the

**Table 3**  
Density and porosity of the examined ceramic disks.

	Density (kg/m <sup>3</sup> )			Porosity (%)		
	550 °C	850 °C	1050 °C	550 °C	850 °C	1050 °C
PIK-UT	1830	1830	1780	32	32	33
PIK-G10	1880	1830	1820	30	31	32
PIK-G40	1870	1830	1810	29	31	32
PIK-P10	1880	1860	1810	30	31	33
PIK-P40	1920	1840	1810	30	33	34
KAL-UT	1830	1850	2470	34	33	11
KAL-G10	1870	1910	2400	32	31	13
KAL-G40	1870	1880	2090	31	30	22
KAL-P10	1850	1830	2450	33	34	12
KAL-P40	1890	1900	2260	32	32	19

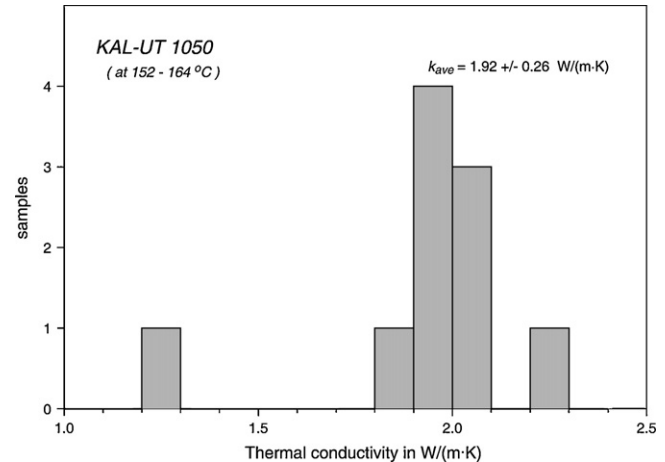


**Fig. 3.** Repeatability of the measurement. The thermal conductivity of Sample KAL-UT-1050 (non-tempered Kalami clay fired at 1050 °C) was determined in 10 independent measurements at a temperature of 164 °C on the heating plate.

same temperatures indicated that the measured temperature differences can vary in a range of up to  $\pm 2$  °C, which assumedly can be explained by variations in the ambient temperature but also by possible incomplete contacts at the ceramic surfaces or the thermocouples. In extreme cases the measured surface temperature was clearly too low. The measured temperature difference, however, appears to be the main error source for the calculated thermal conductivity. The effect of the uncertainty of the temperature difference on the determined thermal conductivity is higher when the temperature differences are small. This is the case at low temperatures of the heating source or at high thermal conductivities.

In order to estimate the long-term precision of the measurements, the thermal conductivity of ceramic disk KAL-UT-1050 was measured 10 times in a period of several months and the results are presented in Fig. 3. Nine out of 10 measurements showed temperature differences between 12 °C and 15 °C. Only in one case the temperature difference measured was 20 °C, resulting in a significantly lower estimation of the thermal conductivity. This value is obviously a result of incomplete heat contact but it shows that if the measurements are repeated at least once it is likely to detect such inconsistencies.

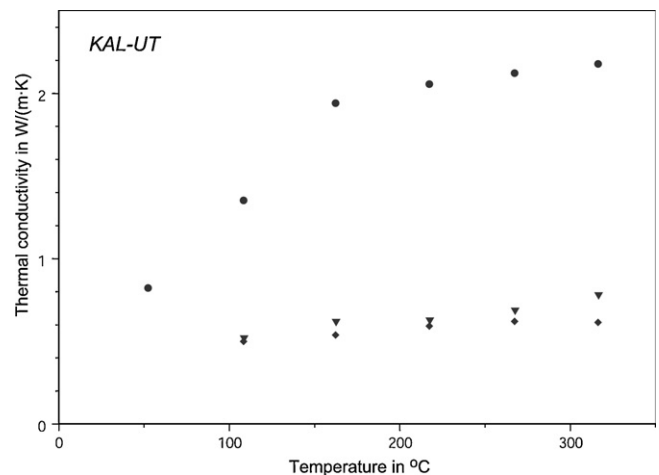


**Fig. 4.** Thermal conductivity of the disks from the non-tempered Kalami clay. The symbols correspond to the firing temperatures: (◆) 550 °C, (▼) 850 °C and (●) 1050 °C.



### 5.1. Influence of firing temperature and clay type

Fig. 4 presents the determined thermal conductivities of the non-tempered Kalami clay KAL-UT fired at different temperatures. For all three firing temperatures the thermal conductivity appears to increase with increasing temperature at least in the observed temperature range. The ceramic disk fired at 1050 °C has a clearly higher thermal conductivity, which is probably related to the relatively dense glass filament network developed in its mass and its therefore lower porosity in comparison with the lower fired specimens of the same base clay (Fig. 5). This difference, however, cannot be explained with the effect of porosity only. According to Eq. (2) porosity of 11% in the case of KAL-UT-1050 in comparison to 33% in

the case of KAL-UT-850, would result in effective thermal conductivities  $k_{eff}$  of 84% of and of 55%, respectively, with regard to  $k_{solid}$ . The measured values, however, show a factor of approximately 3 between the effective thermal conductivity of KAL-UT-1050 and KAL-UT-850 (Fig. 4). Therefore, other effects, such as differences of the ceramic microstructure or the formation of new high temperature phases have to be taken in account as well. According to XRD, predominant phases in KAL-UT-1050 are quartz, hematite and mullite, all presenting a considerably high thermal conductivity [19]. There also appears to be a small increase in thermal conductivity between the disk fired at 550 °C and that fired at 850 °C.

The behaviour of the other clay type, the non-tempered calcareous Pikermi clay PIK-UT, was in general similar to KAL-UT, in terms

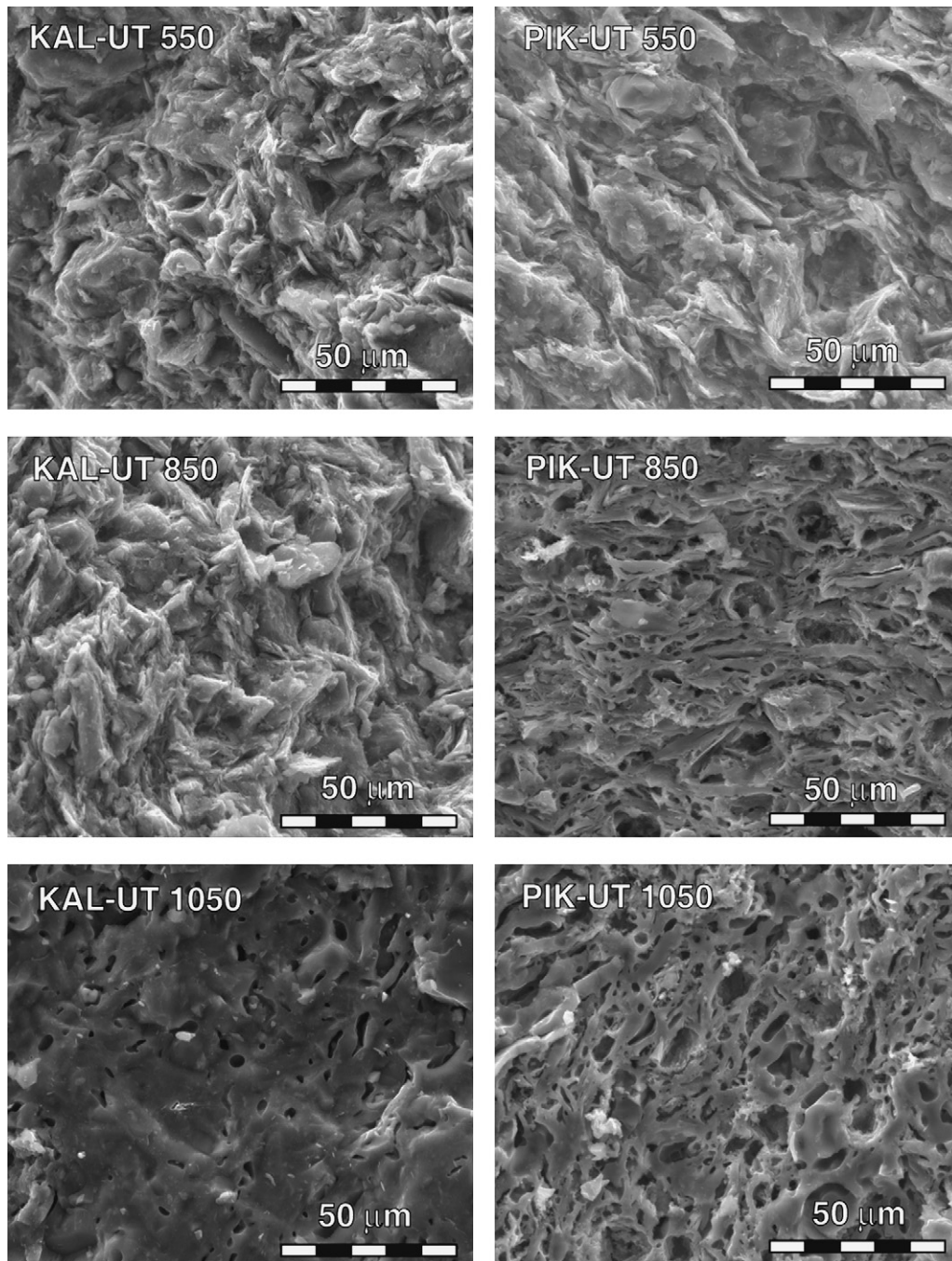
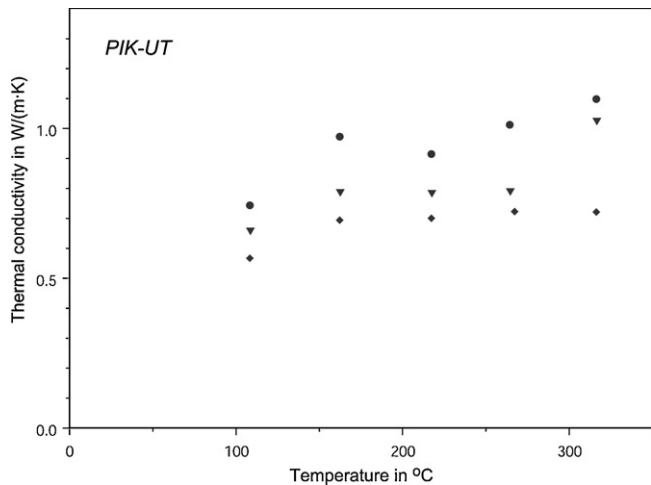


Fig. 5. SEM photomicrographs demonstrating the degree of vitrification observed in the non-tempered Kalami and Pikermi clays fired at 550 °C, 850 °C and 1050 °C.



**Fig. 6.** Thermal conductivity of the disks from the non-tempered Pikermi clay. The symbols correspond to the firing temperatures: (◆) 550 °C, (▼) 850 °C and (●) 1050 °C.

of increase of thermal conductivity with firing temperature (Fig. 6). However, there was a quantitative difference regarding the values of thermal conductivity, most prominently the lower value of the disk fired at 1050 °C compared to the respective KAL-UT disk. Furthermore, the scale of increase is different in the two clays, as can be seen in Figs. 4 and 6. It is worth noting that, although in KAL-UT specimens the thermal conductivities of the samples fired at 550 °C and 850 °C are similar while the one fired at 1050 °C is significantly higher, in PIK-UT there are consistent, but smaller differences among the three firing temperatures curves (Figs. 4 and 6). In the case of the non-tempered Pikermi clay, the correlation between thermal conductivity and firing temperature clearly is not related to porosity, which is approximately the same for all firing temperatures (Table 2). Also in this case, new forming mineral phases, mainly hematite, might be the decisive factor, albeit not to the same extent as in the Kalami clay.

The differences in the thermal behaviour of the two clays can be explained by considering the microstructures developed at each temperature which are typical for these clay types [20]. More specifically, the low calcareous KAL-UT exhibits no vitrification at

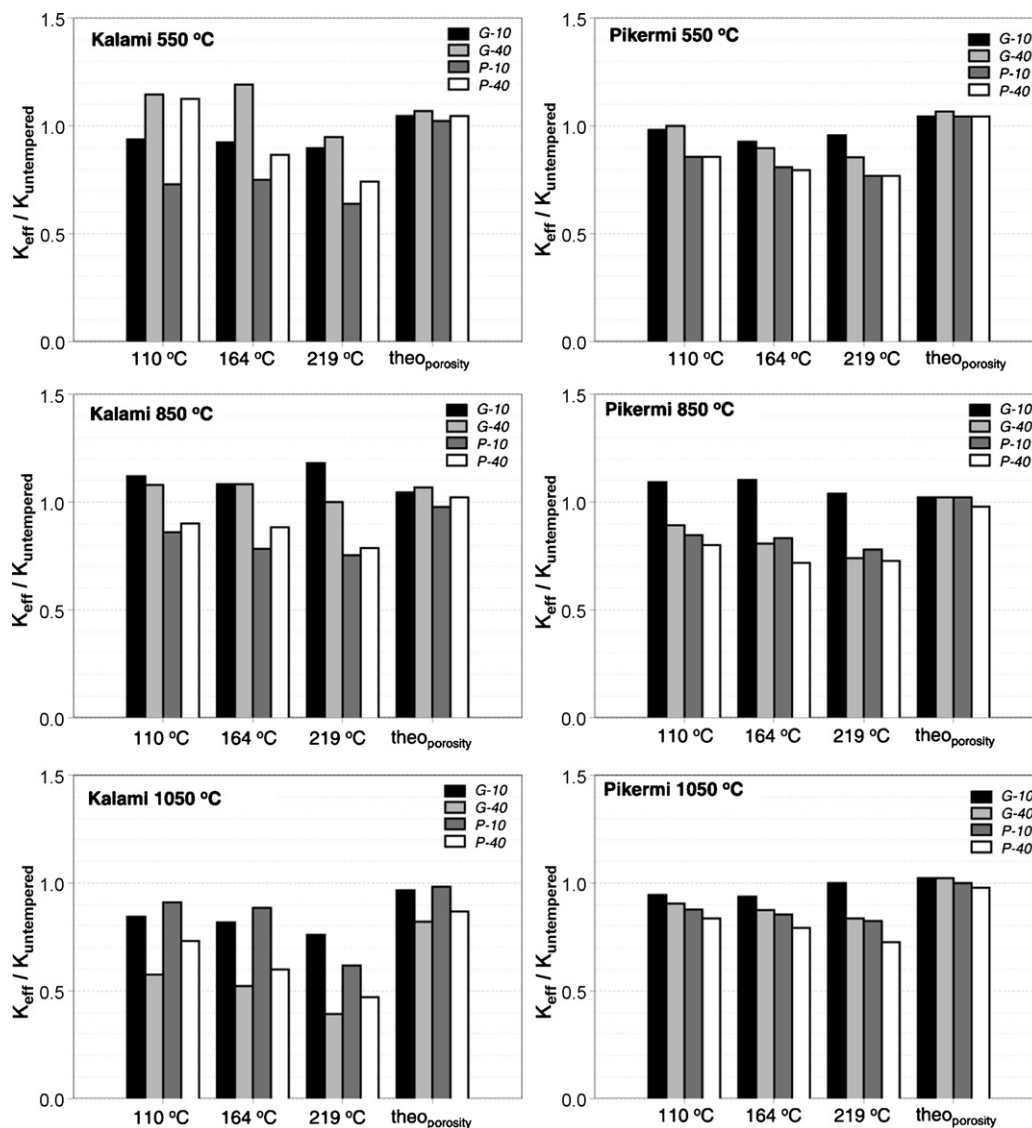


**Fig. 7.** Ratios of the measured effective thermal conductivity  $k_{eff}$  of the tempered clays and the thermal conductivity of the non-tempered clays fired at 550 °C, 850 °C and 1050 °C. Values are presented for three different temperatures of the heating plate. Furthermore, theoretical ratios are presented which correspond to the change of thermal conductivity considering the differences in porosity.

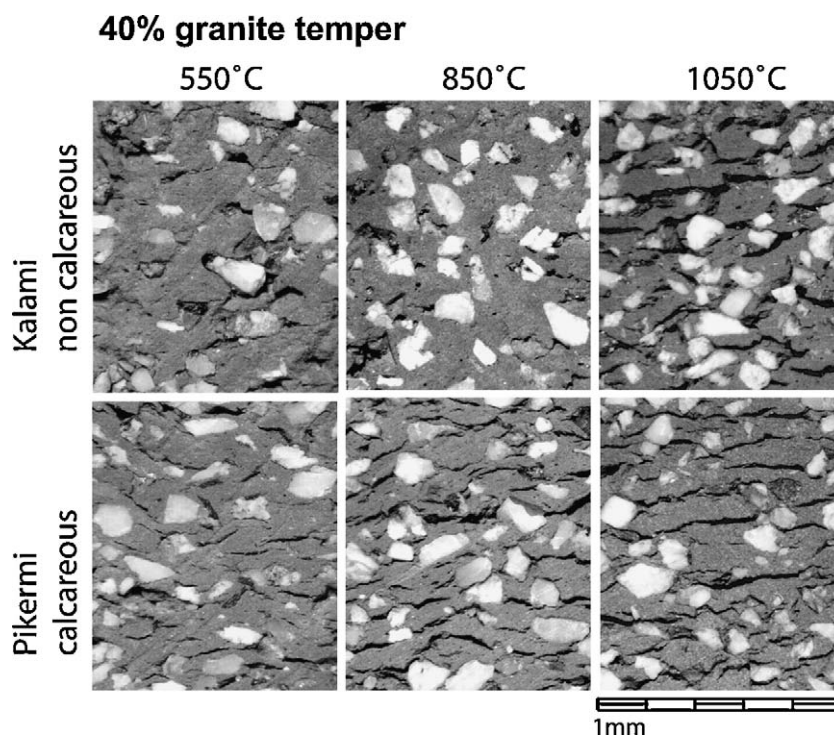


**Fig. 8.** Effect of 40% granite tempering on the microstructure of the two base clays fired at different temperatures. Originating from the granite inclusions, cracks develop with preferred orientation perpendicular to the direction of the heat transfer, which is presumably from top to bottom. It is noticeable that the cracks in the Kalami-based mixture emerge only at 1050 °C, while the development of cracks in the Pikermi-based mixture appears more consistent across different temperatures.

550 °C, some traces at 850 °C, but at 1050 °C the microstructure is characterised by extensive areas of solid glass and therefore lower amounts of pores. In PIK-UT, a highly calcareous clay, there is no vitrification at 550 °C, incomplete vitrification of cellular structure at 850 °C and complete vitrification, but still cellular at 1050 °C, resulting in three microstructures containing considerable amounts of pores (Fig. 5).

### 5.2. Influence of temper material

The effect of tempering on the thermal conductivity  $k$  of the laboratory specimens is presented graphically with the histograms of Fig. 7. Each of the bars represents the ratio of the specimen's thermal conductivity over the one of the non-tempered respective base clay. In other words the ratio provides an estimate of  $k$  variation when clay is tempered with 10 and 40% of granite or phyllite and fired at the three selected temperatures. The four last bars in each histogram represent theoretical values considering the differences only in the measured porosity between tempered and non-tempered specimens and not the mineralogical composition (Table 2). The general impression given in Fig. 7 is that granite inclusions increase the thermal conductivity of the pastes, as in most cases for the 550 °C and 850 °C firing temperatures, the ratio appears higher than 1. On the other hand the respective phyllite tempered specimens appear with ratios lower than 1, indicating the negative effect of this material on thermal conductivity.

The observed differences between granite and phyllite tempering appear to be related to the nature of the inclusions. Whereas granite, a plutonic rock with low porosity, presents commonly a thermal conductivity clearly higher than  $1.5 \text{ W}(\text{m K})^{-1}$ , depending on its feldspar content, the thermal conductivity of phyllite can be smaller especially when the direction of the heat transfer is perpendicular to the main orientation of the sheet silicates [19]. Indeed, during the fabrication of the ceramic disks for the present experi-

ments, care was taken so that the phyllite inclusions were oriented parallel to the surfaces of the ceramic disks, as is the case in the majority of such archaeological fabrics. At least in the case of the ceramics with 10% temper and fired at 550 °C or 850 °C the inclusions appear to be part of the matrix and thus directly affect the effective thermal conductivity  $k_{\text{eff}}$  of the mixture. According to this assumption in the case of 40% granite temper a further increase of  $k_{\text{eff}}$  would be expected. That this is not the case can be explained by the fact that a high amount of non-plastic inclusions induces discontinuities in the clay matrix during manufacture. The rigid particles act as a skeleton, hindering the overall shrinkage of the sample and thus inducing extra porosity during drying and firing (Fig. 8). This extra porosity obscures the possible increase of  $k$  due to granite and, as can be seen in Fig. 7, reduces the ratios compared to the 10% values.

The high fired ceramics show a different picture. In the case of the tempered Kalami clay the thermal conductivity is clearly reduced with both tempers, although in terms of absolute values the thermal conductivity is still quite high compared to the Pikermi samples. At these temperatures the vitrified bodies exhibit dense vitrification which results in an increase in thermal conductivity of the ceramic material, probably in the same range as the granite inclusions. These therefore do not increase further  $k_{\text{eff}}$  as is the case in the lower fired ceramics. At the same time in the high fired Kalami specimens the determined porosity increases considerably with tempering (Table 2), which also explains the observed decrease of  $k$ . However, if this was the only reason for the decrease, then the theoretical values for the high fired Kalami-based mixtures (Fig. 7) should be similar to the experimental. To account for the differences observed between theoretical and experimental values, a further effect needs to be considered, particularly in the case of granite tempering: this is the formation of elongated cracks during firing, originating from the inclusions and acting as heat barriers (Fig. 8). Due to the manufacturing process of the ceramic



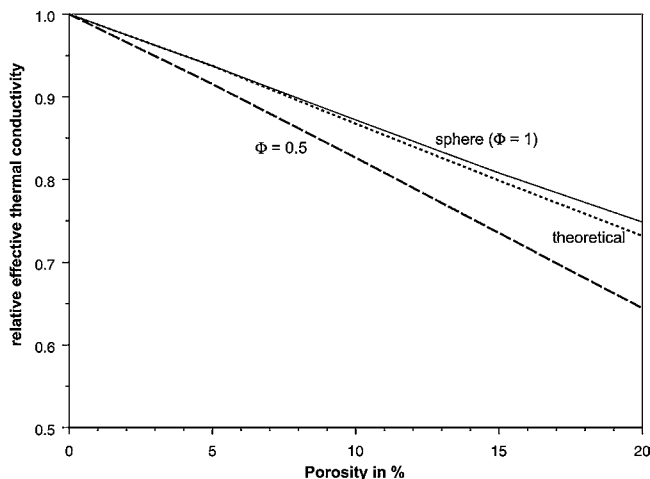


**Fig. 9.** Influence of pore shape on relative effective thermal conductivity. Presented here is the decrease of thermal conductivity correlated to porosity as calculated by finite element analysis [1] for unit cells with spheroid pores. Two cases were examined, a sphere and an oblate spheroid ( $\Phi = 0.5$ ) with heat flux parallel to the rotation axis ( $\theta = 0^\circ$ ). For comparison the theoretical relative effective thermal conductivity is included (Eq. (2)).

disks the cracks are oriented perpendicular to the heat flux, which additionally decreases the thermal conductivity [1]. For illustration, the effect of pore shape has been simulated (Fig. 9), comparing spherical pores with oblate shaped pores oriented with their rotation axis parallel to the heat flux. It is obvious that apart from the absolute porosity, shape and orientation of the voids can affect thermal conductivity in a range which explains the extreme decrease of thermal conductivity in the high fired Kalami clay. As for the high fired Pikermi clay the reducing effects of the tempering on the thermal conductivity are not as severe as in the Kalami clay. This can be explained with the originally lower thermal conductivity of the non-tempered clay and with the lower degree of vitrification in comparison with the non-calcareous clay.

In conclusion, the addition of temper appears not to be particularly beneficial for the thermal conductivity of the ceramics. There are many parameters affecting the thermal conductivity of the mixtures, besides the materials themselves, the most important being the size and the shape of the cracks introduced during manufacture. In fact granite tempering up to a moderate volume fraction increases thermal conductivity, but when it exceeds the 20–30% range it induces elongated pores. Tempering with phyllites in general reduces the thermal conductivity due to its platy shape. Indeed, granite and quartz temper have been used extensively in cooking ware in the Mediterranean and elsewhere. Also the import of granitic cooking ware to the Bronze Age settlement of Akrotiri on the volcanic island of Santorini, Greece, where such materials were not available locally, can be viewed in the light of their enhanced thermal properties. On the other hand, the similarly observed use of phyllites seems to have been linked rather to advantages related to the vessels' strength levels, as the vessels concerned were usually fired to rather high temperatures. Focussing only on optimum heat transfer conditions, ceramics should have been non-calcareous, fired at sufficiently high temperatures and containing moderate amounts of temper. The archaeological evidence, however, shows that cooking ware was rarely fired at temperatures considerably higher than  $850^\circ\text{C}$  and that both clay types, calcareous and non-calcareous, were used. Therefore, when these findings are utilized for the understanding of the performance of pottery, other material properties should be included in the consideration, such as strength and toughness as well as parameters not related to function, such as tradition and cultural influences.

## 6. Conclusions

The presented measurements of experimental ceramic disks demonstrated the suitability of the applied Lees' disk setup to determine thermal conductivity of archaeological or traditional ceramics with sufficient precision and also with reasonable accuracy. In this way archaeological and other earthenware ceramics can be examined for their thermal properties, using either sample replicates as in the presented case or samples cut from actual archaeological ceramic fragments, which will be the next step. In either case conclusions can be drawn from these results concerning the selection of certain raw materials or the application of particular fabrication techniques in order to produce ceramics with suitable thermal properties. Furthermore, the reference values determined for the thermal properties of archaeological ceramics can be used in computer models simulating the performance of the ceramics during use.

For the specific case of the use of granite and phyllite as tempers in cooking vessels, it has been demonstrated that their presence affects thermal properties but in different ways. Moderate amounts of granite increase thermal conductivity while the addition of phyllite generally results in a reduction of this property due to its platy arrangement and anisotropic nature. These findings contribute to our understanding of materials choices by potters of the past, in view of technological developments in the ancient world.

## Acknowledgements

The authors would like to thank Th. Ioannidis from XENON for the collaboration concerning the development and maintenance of the Lees' disk device. This study was partly funded by the Institute for Aegean Prehistory (INSTAP). The support of one of us (NM) through an IKY (Greek State Scholarship Foundation) scholarship is gratefully acknowledged, as is an ORSAS Scholarship awarded by Universities UK.

## References

- [1] A. Hein, V. Kilikoglou, *J. Am. Ceram. Soc.* 90 (3) (2007) 878–884.
- [2] M. Tite, V. Kilikoglou, G. Vekinis, *Archaeometry* 43 (2001) 301–324.
- [3] S.M. West, *Temper, thermal shock and cooking pots: a study of tempering materials and their physical significance in prehistoric and traditional cooking pottery*, Unpublished MSc Thesis, University of Arizona, Tucson, 1992.
- [4] J.M. Skibo, M.B. Schiffer, K.C. Reid, *Am. Antiquity* 54 (1) (1989) 122–146.
- [5] M.S. Tite, V. Kilikoglou, A. Hein, Y. Maniatis (Eds.), *Modern Trends in Scientific Studies on Ancient Ceramics*. BAR International Series 1011, Archaeopress, Oxford, 2002, pp. 1–8.
- [6] T. Broekmans, A. Adriaens, E. Pantos, *Nucl. Instrum. Method B* 226 (1–2) (2004) 92–97.
- [7] D. Braun, in: J.A. Moore, A.S. Keene (Eds.), *Archaeological Hammers and Theories*, Academic Press, New York, 1983, pp. 107–134.
- [8] M.B. Schiffer, *J. Archaeol. Sci.* 17 (1990) 373–381.
- [9] C. Pierce, *J. Archaeol. Method Theory* 12 (2) (2005) 117–157.
- [10] S.K. Hannani, E. Hessari, M. Fardadi, M.K. Jeddi, *Energy* 31 (2006) 2969–2985.
- [11] W.D. Kingery, W.H. Gourdin, *J. Field Arch.* 3 (1976) 351–353.
- [12] M.S. Tite, M.J. Hughes, I.C. Freestone, N.D. Meeks, M. M. Bimson, in: B. Rothenberg (Ed.), *The Ancient Metallurgy of Copper*, Institute for Archaeometallurgical Studies, London, 1990, pp. 158–175.
- [13] I.C. Freestone, in: A. Hauptmann, E. Pernicka, G.A. Wagner (Eds.), *Archaeometallurgie der Alten Welt—Old World Archaeometallurgy*, Der Anschnitt Beiheft 7, Deutsches Bergbau Museum, Bochum, 1989, pp. 155–162.
- [14] W.D. Kingery, H.K. Bowen, D.R. Uhlmann, *Introduction to Ceramics*, 2nd edition, John Wiley & Sons, New York, 1976.
- [15] E.Y. Litovsky, M. Shapiro, *J. Am. Ceram. Soc.* 75 (12) (1992) 3425–3439.
- [16] V. Kilikoglou, G. Vekinis, Y. Maniatis, P.M. Day, *Archaeometry* 40 (2) (1998) 261–279.
- [17] F.H. Chung, *J. Appl. Crystallogr.* 7 (1974) 519–525.
- [18] EN 993-1, *European Standards, Methods for dense shaped refractory products. Part 1. Determination of bulk density, apparent porosity and true porosity*, 1995.
- [19] C. Clauser, E. Huenges, in: T.J. Ahrens (Ed.), *Rock Physics and Phase Relations: A Handbook of Physical Constants*, American Geophysical Union, Washington, 1995, pp. 105–126.
- [20] Y. Maniatis, M.S. Tite, *J. Archaeol. Sci.* 8 (1981) 59–76.